

SOME NEW RESULTS IN INVERSE RECONSTRUCTION.

Alfred S. Carasso, ACMD.

PART I

**FALSE RECONSTRUCTIONS FROM
IMPRECISE DATA IN PARABOLIC
EQUATIONS BACKWARD IN TIME**

REFERENCE: NISTIR # 7783.

To appear in

Mathematical Methods in the Applied Sciences

Identify sources of groundwater pollution

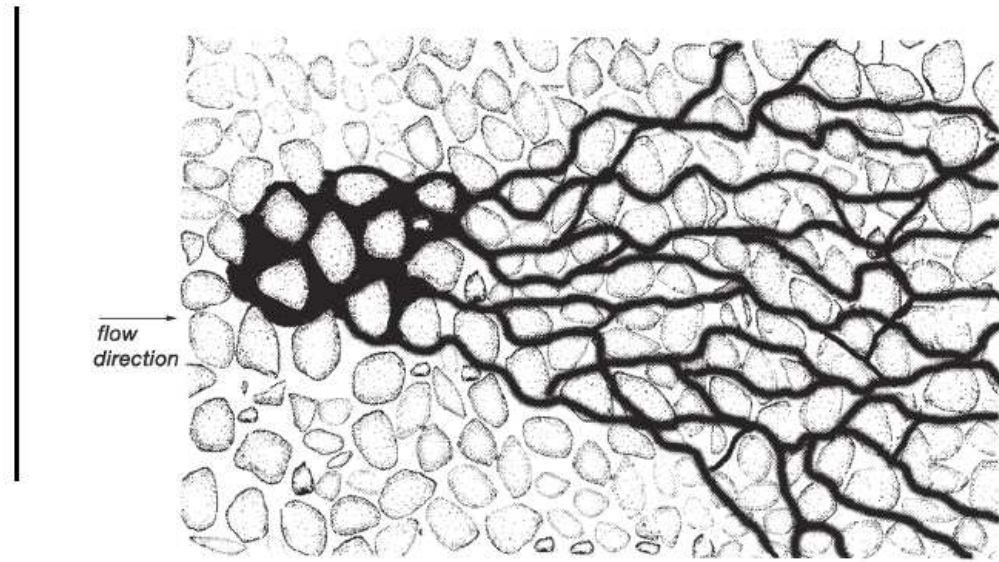


Fig.1 Contaminant transported in porous media

Solve Advection Dispersion Equation backward in time, given present state $g(x, y)$:

$$C_t = \nabla \cdot \{D \nabla C\} - \nabla \cdot \{vC\}, \quad 0 < t \leq T,$$

$$C(x, y, T) = g(x, y).$$

(1)

DEBLURRING GALAXY IMAGES HUBBLE SPACE TELESCOPE; (ACS CAMERA)

Original NGC 1309



Logarithmic diffusion



Solve logarithmic diffusion equation backward in time, given blurred image $g(x, y)$:

$$w_t = - \left[\lambda \log \{ 1 + \gamma (-\Delta)^\beta \} \right] w, \quad 0 < t \leq T,$$
$$w(x, y, T) = g(x, y).$$

(2)

Logarithmic Convexity Arguments \Rightarrow Backward Uniqueness and Stability

Well-posed parabolic eq. $w_t = Lw$, $0 < t \leq T$,
in $L^2(\Omega)$, with **negative self adjoint** spatial
operator L , so that $(w, Lw) = (Lw, w) \leq 0$.

Let $F(t) = \|w(\cdot, t)\|^2$. Show $\log F(t)$ con-
vex function of t , $\iff d^2/dt^2\{\log F(t)\} \geq 0$.

Must show $FF'' - (F')^2 \geq 0$. $F'(t) = 2(w, Lw)$;
 $F''(t) = 2(w_t, w_t) + 2(w, w_{tt}) = 2(Lw, Lw) +$
 $2(w, L^2w) = 4 \|Lw\|^2$. Schwarz's inequality
 $\implies (F')^2 = 4|(w, Lw)|^2 \leq 4 \|w\|^2 \|Lw\|^2$.
Hence, $FF'' - (F')^2 \geq 0$. QED.

$\Rightarrow \|w(\cdot, t)\| \leq \|w(\cdot, 0)\|^{(T-t)/T} \|w(\cdot, T)\|^{t/T}$.

Non Selfadjoint or Nonlinear \Rightarrow

$FF'' - (F')^2 \geq -kFF'$, $k > 0$. Now, with $\sigma = e^{-kt}$, $\log F(t)$ is a convex function of σ .

Ex. **Navier-Stokes eqns** (Knops-Payne 1968)

Well-posed linear or nonlinear parabolic equation $w_t = Lw$ on $0 < t \leq T$, with approx data $f(x)$ at time T such that $\|w(\cdot, T) - f\| \leq \delta$.

Using $f(x)$, find solution $w(x, t)$, $0 \leq t \leq T$, such that $\|w(\cdot, 0)\| \leq M$, ($\delta \ll M$).

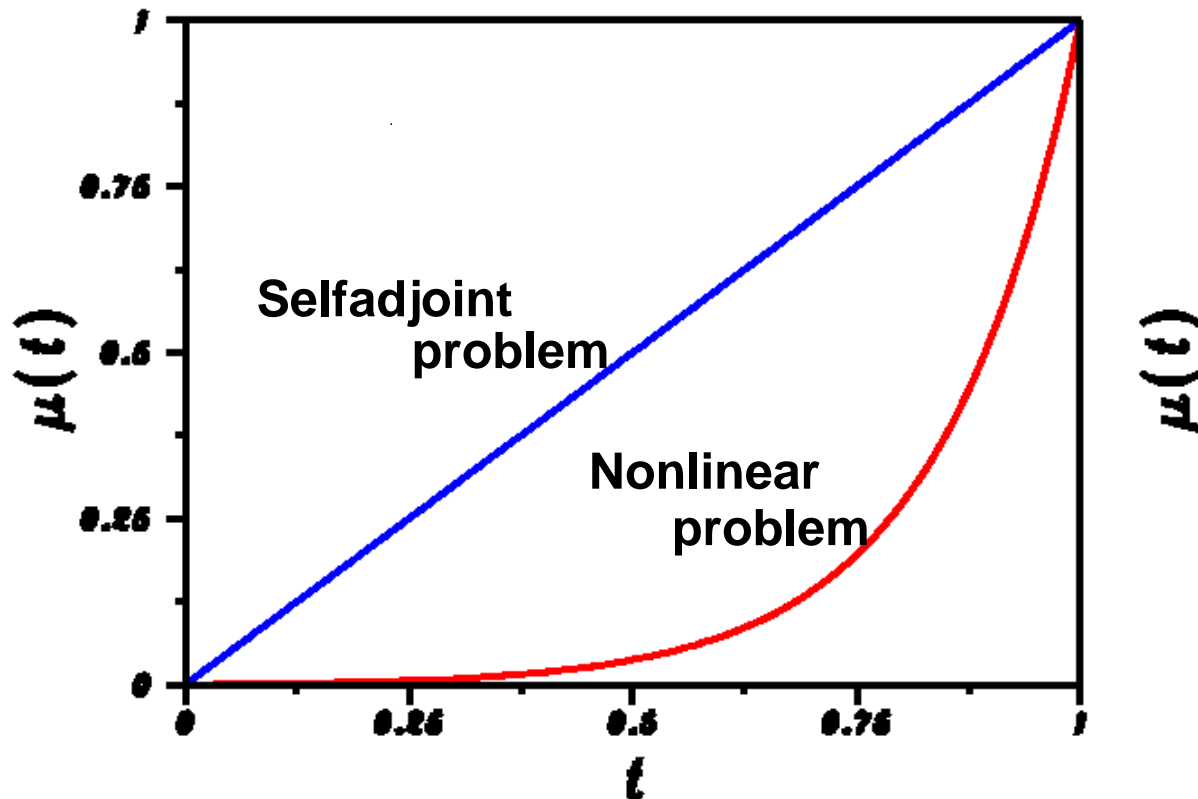
If $w^1(x, t), w^2(x, t)$ are any two solutions, then

$$\|w^1(\cdot, t) - w^2(\cdot, t)\| \leq 2M^{1-\mu(t)}\delta^{\mu(t)}, \quad 0 \leq t \leq T.$$

Here, $\mu(t) = (1 - e^{-kt})/(1 - e^{-kT})$, $\mu(T) = 1$, $\mu(0) = 0$, with $\mu(t) > 0$, $t > 0$, and $\mu(t) \downarrow 0$ as $t \downarrow 0$. **Implies backward uniqueness, but no guaranteed accuracy at $t = 0$, even with very small $\delta > 0$.**

Difficulty of backward reconstruction hinges on behavior of Hölder exponent $\mu(t)$ as $t \downarrow 0$. Selfadjoint problems $\Rightarrow \mu(t) = t/T$. Nonlinear problems $\Rightarrow \mu(t)$ sublinear in t .

Behavior of Holder exponent in backward problems



Van Cittert iteration in backward problem

Forward parabolic initial value problem

$$w_t = Lw, \quad w(x, 0) = h(x), \quad 0 < t \leq T.$$

Forward solution operator S at time T :

$$S[h(x)] = w_h(x, T). \quad \text{Obtained **numerically** .}$$

With approximate data $f(x)$ at time T , and

$h^1(x) = \gamma f(x)$, consider iterative process:

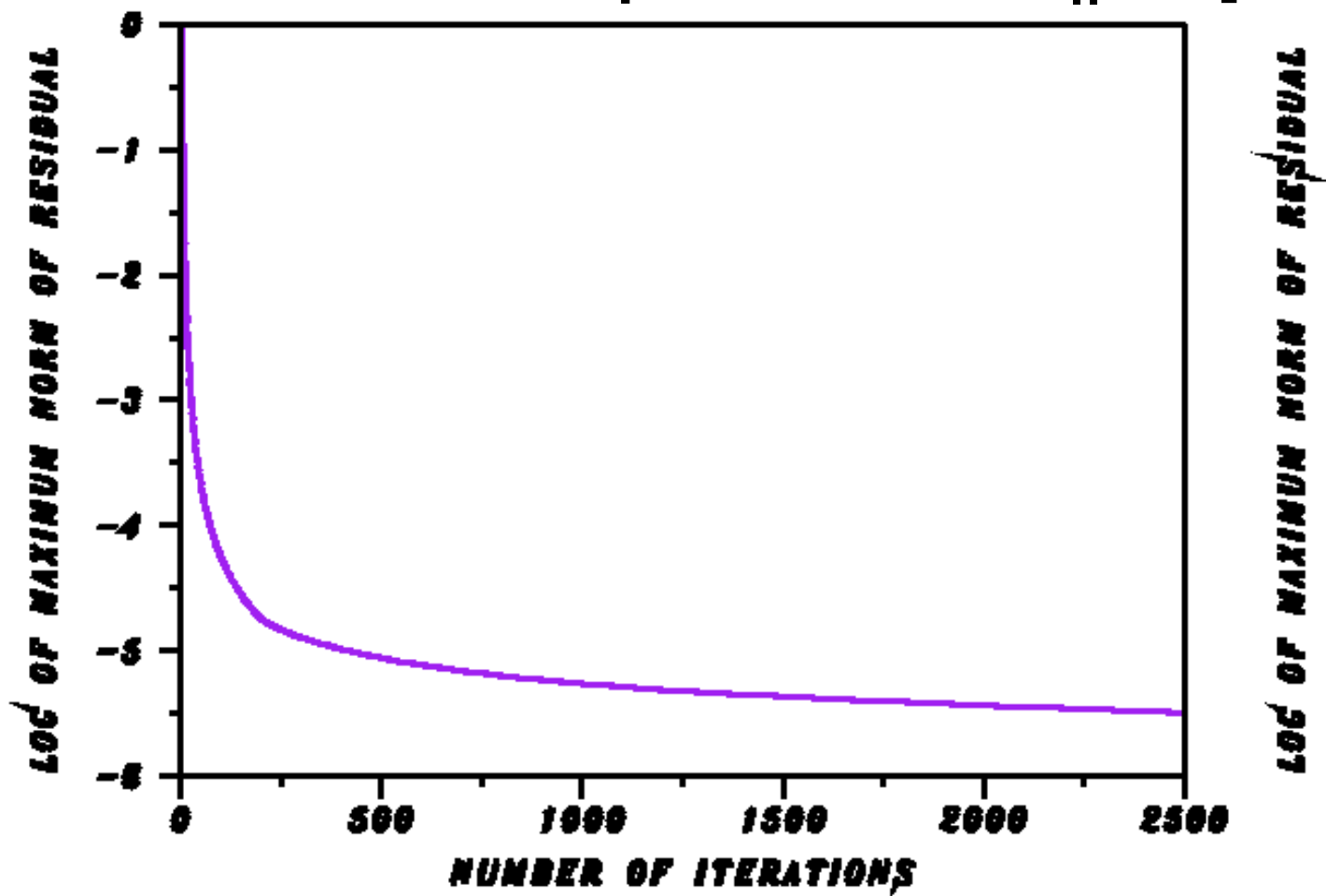
$$h^{n+1}(x) = h^n(x) + \gamma \{f(x) - S[h^n(x)]\}, \quad n \geq 1.$$

Find $\|f - S[h^N]\| \leq \delta$ for some large N .

If $\|h^N\| \leq M$, then $h^N(x)$ is **valid reconstruction** of unknown $w(x, 0)$ from the data $f(x)$.

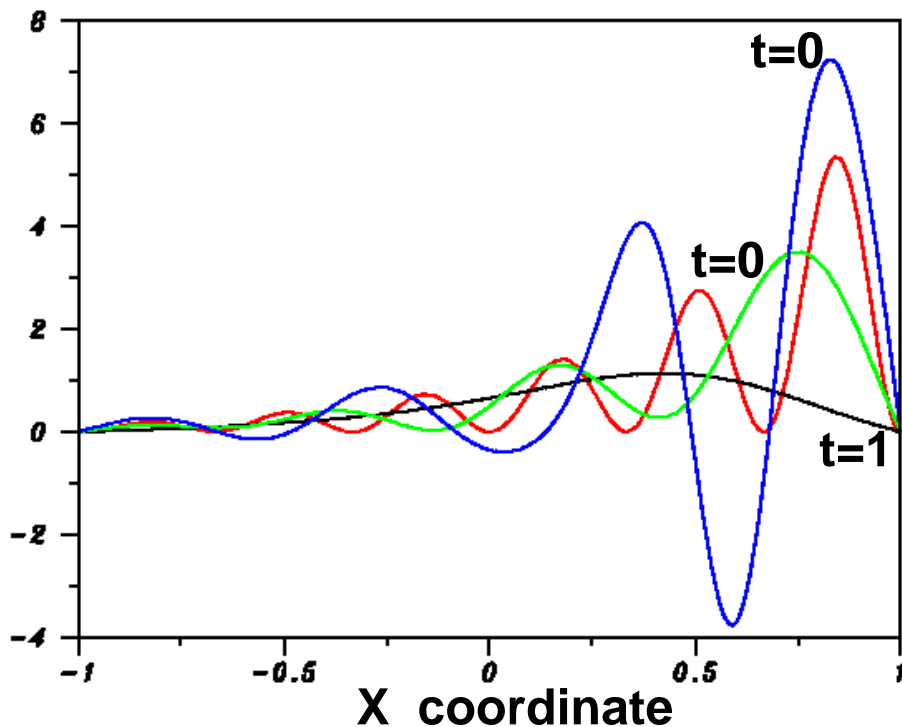
TYPICAL VAN CITTERT BEHAVIOR

Van Cittert iteration in non selfadjoint example.
Behavior in residual supremum norm $\|f - S[h^n]\|$.



Linear non selfadjoint parabolic equation

Effective backward non uniqueness in linear non selfadjoint example.



Each of red, green, or blue initial values at $t=0$, terminates on black curve at $t=1$, to within $4.1E-3$ pointwise, and L2 relative error $2.6E-3$.

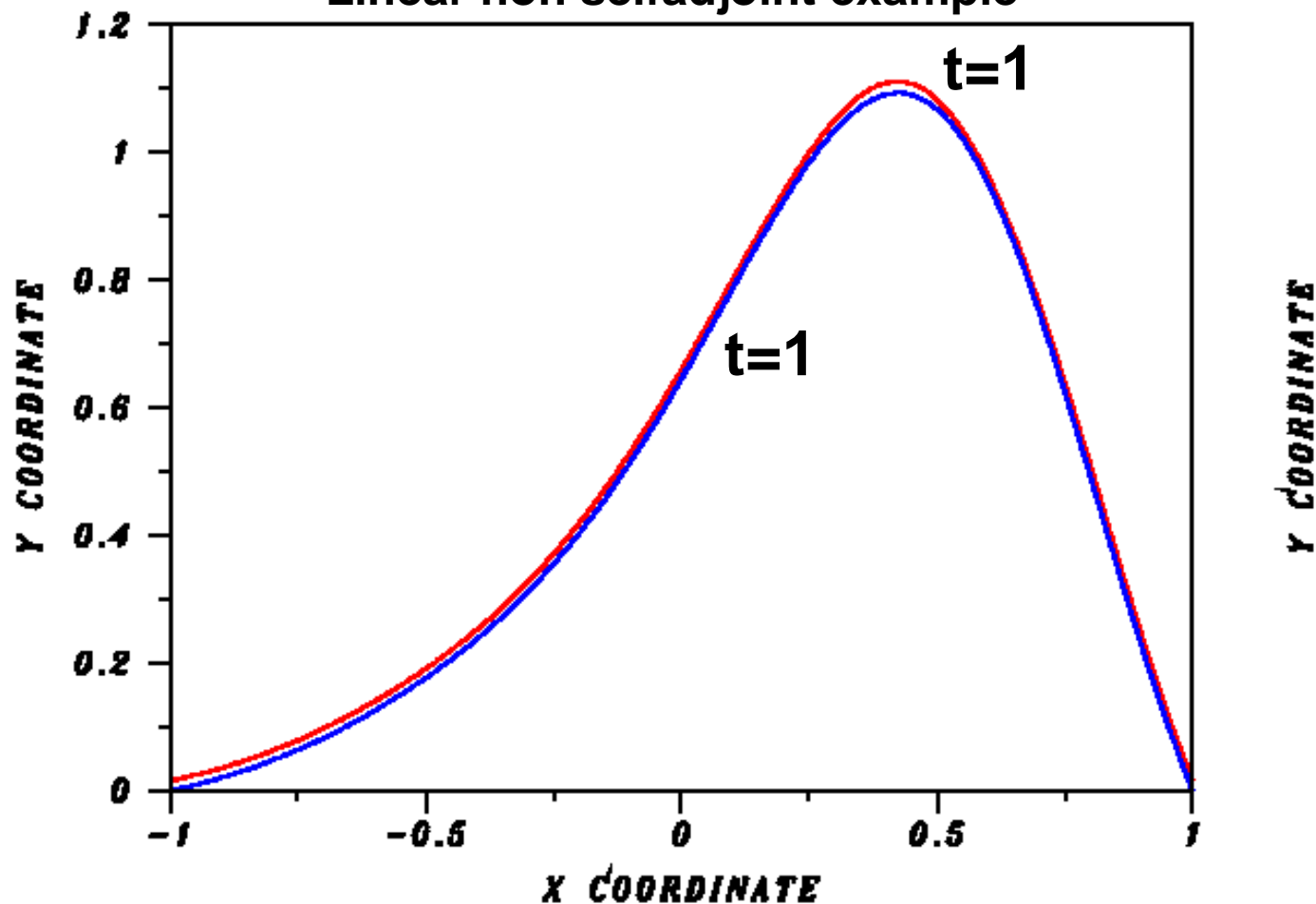
$$w_t = 0.05 \left\{ e^{(0.025x+0.05t)} w_x \right\}_x + 0.25w_x, \quad -1 < x < 1, \quad 0 < t \leq 1.0,$$

$$w(x, 0) = e^{2x} \sin^2(3\pi x), \quad w(-1, t) = w(1, t) = 0, \quad t \geq 0.$$

HOW SOLUTIONS AGREE AT $t=1$

RED AND BLUE SOLUTIONS IN VISUAL AGREEMENT AT TIME $T=1$.

Linear non selfadjoint example

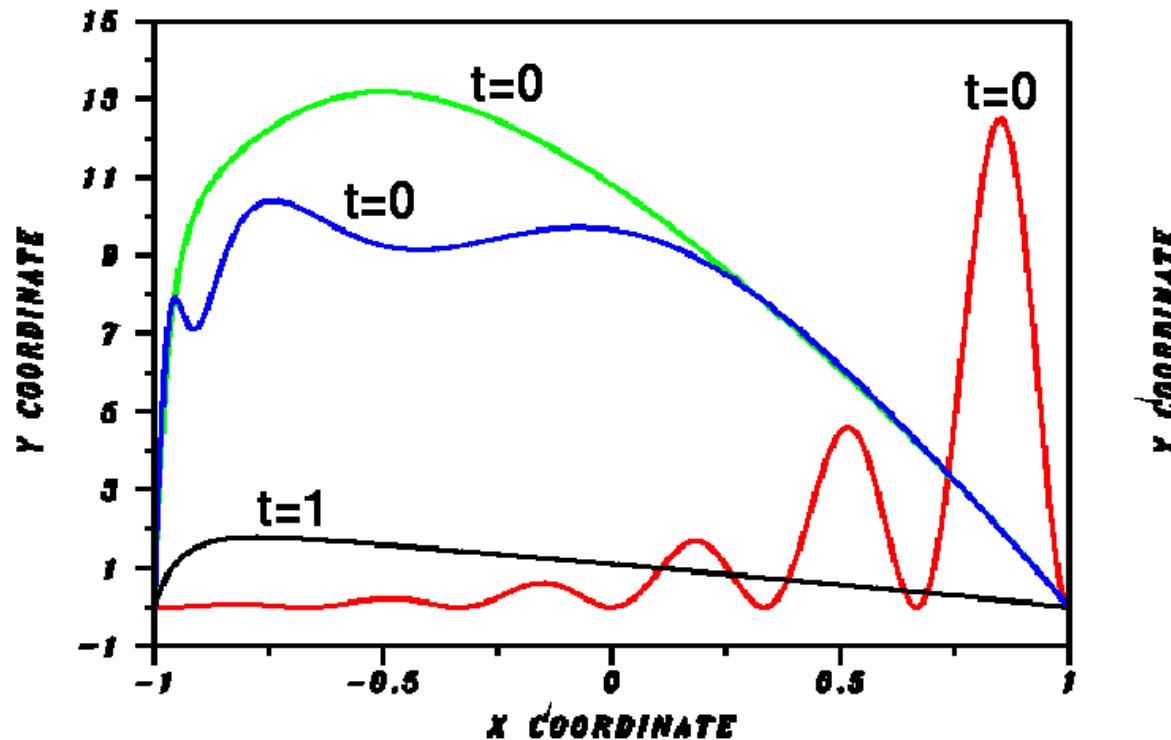


RED CURVE ARTIFICIALLY RAISED TO LIE ABOVE BLUE CURVE

Highly distinct red and blue initial values at $t=0$, visually agree at $t=1$.

Strongly nonlinear parabolic equation

Backward non uniqueness in nonlinear example



Each of red, green, or blue initial values at $t=0$, terminates on black curve at $t=1$ to within $5.6E-2$ pointwise, and $L2$ relative error $3.35E-2$.

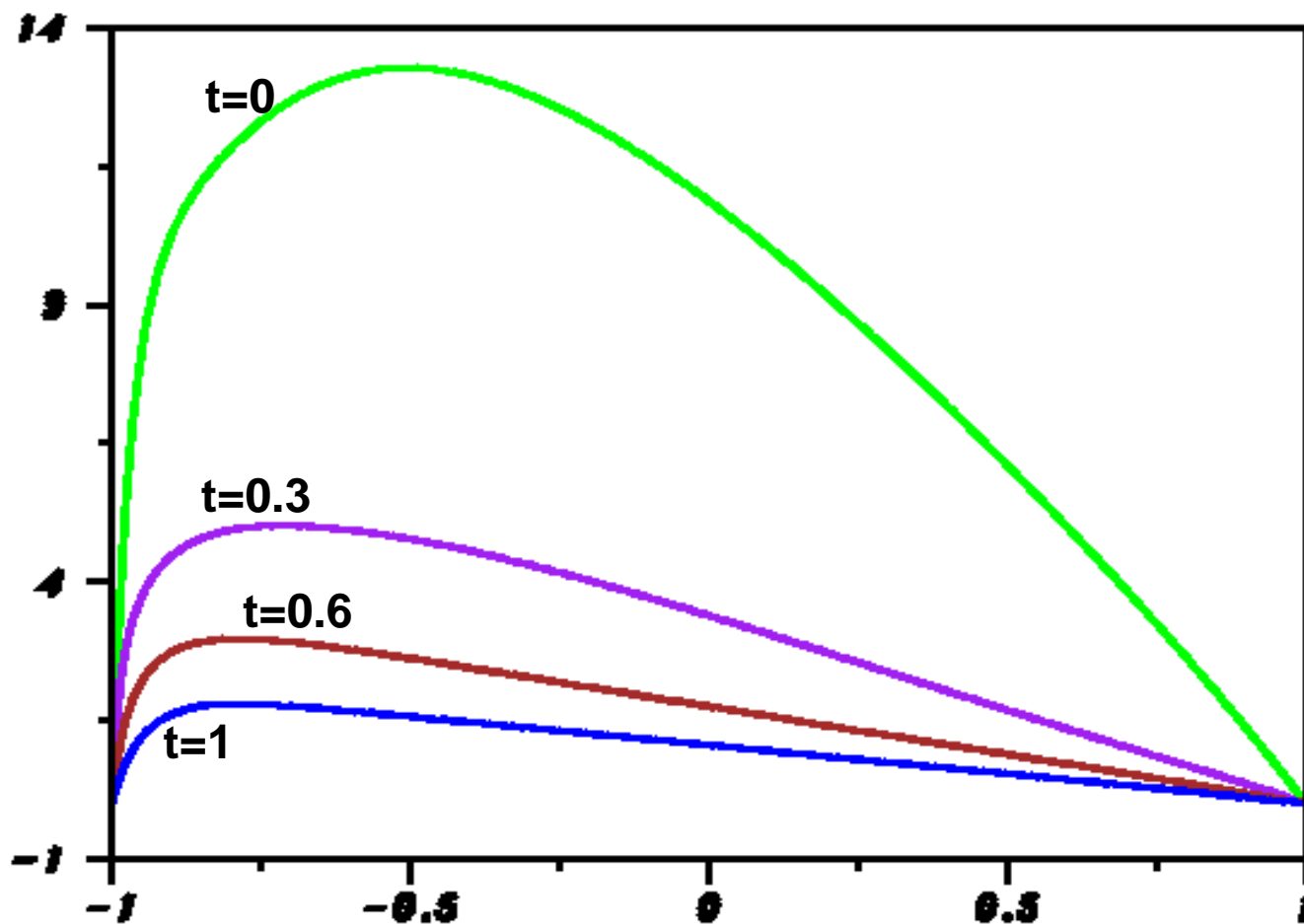
$$w_t = 0.05(e^{0.5w} w_x)_x + w w_x, \quad -1 < x < 1, \quad 0 < t \leq 1.0,$$

$$w(x, 0) = e^{3x} \sin^2(3\pi x), \quad w(-1, t) = w(1, t) = 0, \quad t > 0.$$

(4)

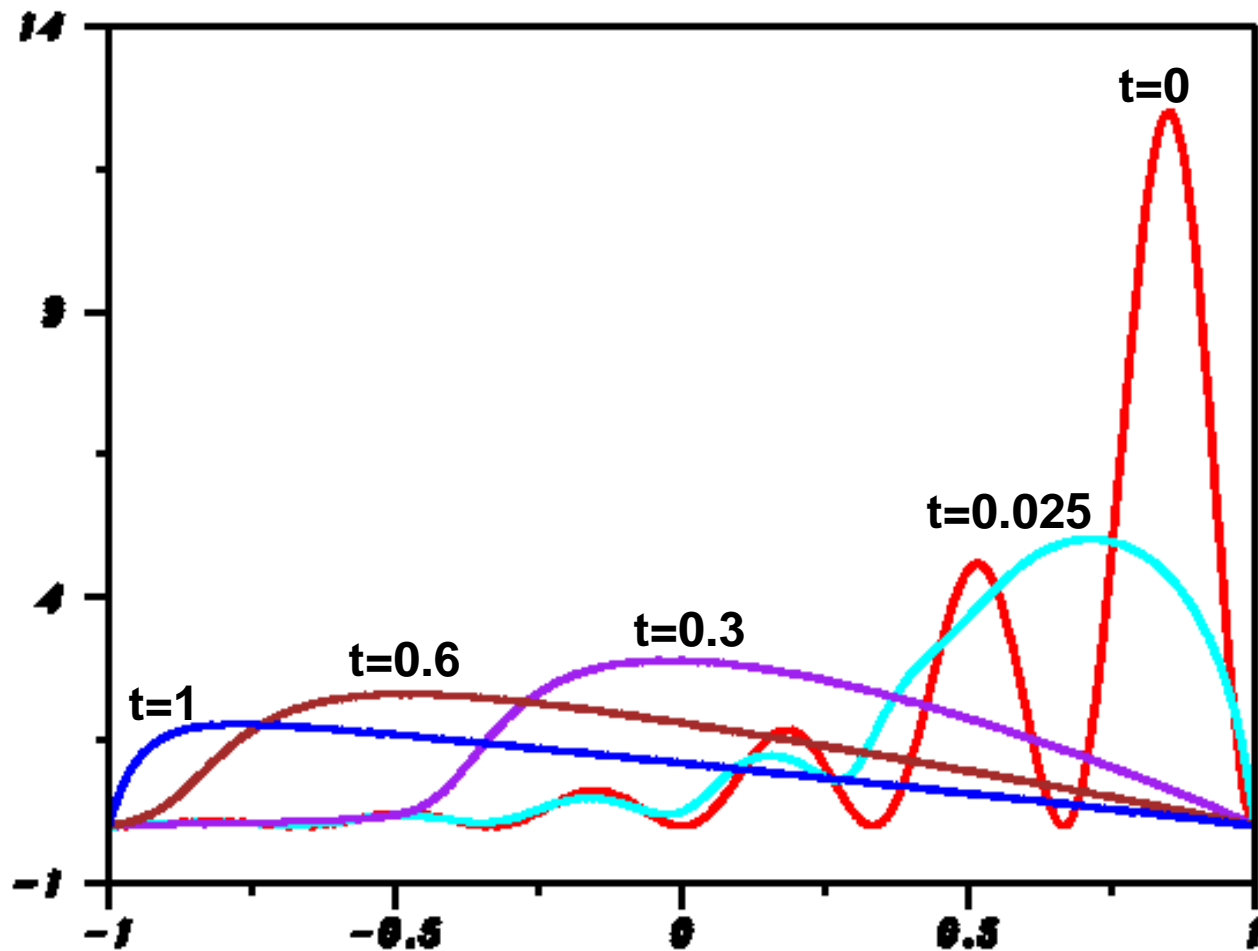
GREEN EVOLUTION; OCCAM'S RAZOR
Simplest Plausible ?? Settled Science ??

EVOLUTION IN NONLINEAR PARABOLIC INITIAL VALUE PROBLEM



LESS PLAUSIBLE RED EVOLUTION ?

EVOLUTION IN NONLINEAR PARABOLIC INITIAL VALUE PROBLEM



Van Cittert iteration. Can be used to find numerous other examples of **false reconstruction** from approximate data.

Multidimensional problems. Very likely a rich source of interesting counterexamples.

Potential impact. Hydrologic Inversion and Image Deblurring.

Detailed prior information on true solution. Necessary to resolve uncertainty in reconstruction.

PART II

**SLOW MOTION DENOISING OF
HELIUM ION MICROSCOPE NANOSCALE
IMAGERY.**

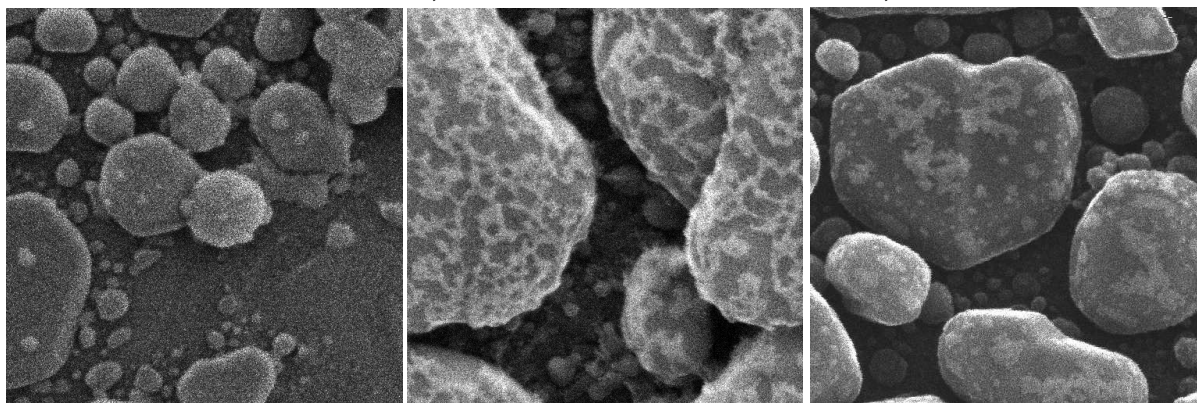
**In collaboration with Andras Vladar, Leader,
NIST Nanoscale Metrology Group**

To appear in

NIST Journal of Research, Jan-Feb 2012

Helium Ion Microscope images are noisy.

ANDRAS VLADAR, NANOSCALE METROLOGY GROUP, NIST.



Smooth by solving fractional diffusion eqn.

$$w_t = -(-\Delta)^\beta w, \quad t > 0, \quad w(\cdot, 0) = g(x, y).$$

Can show $\| \nabla w(\cdot, t) \|_2 = O(t^{-1/2\beta})$, $t \downarrow 0$.

Choose β with $0.1 < \beta < 0.2$.

Blows up fast at $t = 0$. **Suggests** $w_\beta(x, y, t)$ retains fine structure in $g(x, y)$ for small $t > 0$.

Heat eqn ($\beta = 1$) blows up very slowly, $O(t^{-1/2})$.
Smooths out fine structure very quickly.

Use FFT to solve fractional diffusion eqn.

$\hat{w}(\xi, \eta, t) = e^{-t\rho^{2\beta}} \hat{g}(\xi, \eta)$, $t > 0$, with $\rho^2 = (2\pi\xi)^2 + (2\pi\eta)^2$. Inverse Fourier $\Rightarrow w(x, y, t)$.

Conserves L^1 norm: $\|w(\cdot, t)\|_1 = \|g\|_1$, $t > 0$.

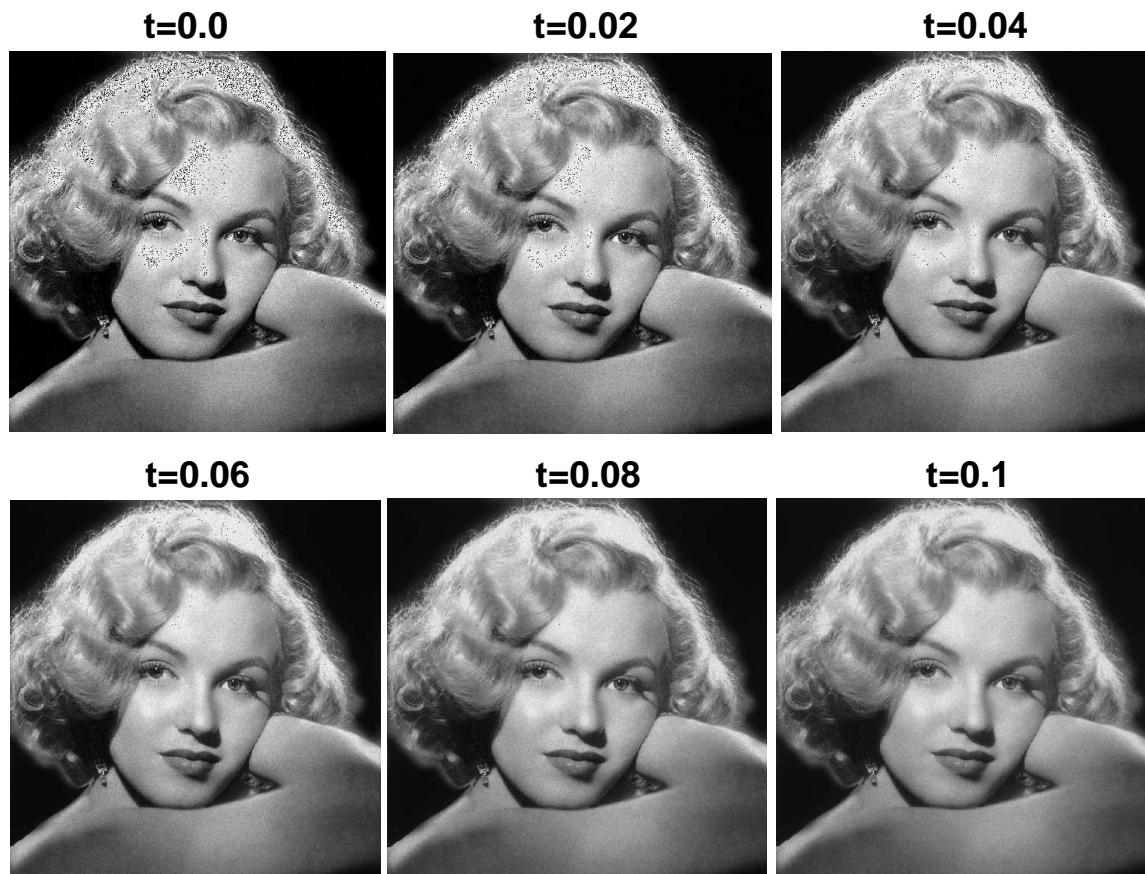
Also, $\|w(\cdot, t) - g\|_2 \uparrow$ **monotonically** as $t \uparrow$,
and $\|\nabla w(\cdot, t)\|_2 \downarrow$ **monotonically** as $t \uparrow$.

Variational Principle: Given noisy image $g(x, y)$,
evaluate $\|\nabla g\|_p$, $p = 1, 2$. **Prescribe** λ with
 $0 < \lambda < 1$. **Define** denoised image $g^L(x, y)$ by

$$g^L = \text{Arg min}_{t>0} \{ \|w(\cdot, t) - g\|_2 \ni \|\nabla w(\cdot, t)\|_2 \leq \lambda \|\nabla g\|_2 \}.$$

Monotonicity $\Rightarrow g^L(x, y) = w(x, y, t^\dagger)$, where
 t^\dagger is earliest time $\ni \|\nabla w(\cdot, t)\|_2 \leq \lambda \|\nabla g\|_2$.

Monitor evolution from noisy $g(x, y)$ at $t = 0$, to denoised $g^L(x, y)$ at $t = t^\dagger = 0.1$.



Rerun with new $\lambda \Rightarrow$ new $t^\dagger \Rightarrow$ new g^L .
 λ controls size of $\|\nabla g^L\|_2 = \lambda \|\nabla g\|_2$.

TOTAL VARIATION (TV) DENOISING

With noisy $g(x, y)$ and regzn parameter $\omega > 0$,
define TV denoised image $g^{tv}(x, y)$ by

$$g^{tv} = \text{Arg min}_{u \in BV(R^2)} \left\{ \|\nabla u\|_1 + \omega/2 \|u - g\|_2^2 \right\}.$$

Assumes true image $\in BV(R^2)$. Denoised
 $g^{tv}(x, y)$ with $\|\nabla g^{tv}\|_1 \ll \|\nabla g\|_1$, **typical !**.

Two good methods for TV denoising: **1. Split Bregman iteration**, and **2. Long time steady-state** solution in Marquina-Osher PDE (Neumann BC; Tunable parameters $\Lambda, \sigma > 0$.)

$$\begin{cases} w_t = -\Lambda |\nabla w| (w - g) + |\nabla w| \nabla \cdot \left(\nabla w / \{\sqrt{|\nabla w|^2 + \sigma}\} \right), \\ w(x, y, 0) = g(x, y), \end{cases} \quad (1)$$

PERONA-MALIK DENOISING

Anisotropic smoothing that retains edges, using diffusion coefficient vanishing at edges.

Consider $dif(u) = 1/(1 + \gamma u^2)$; $\gamma > 0$.

Or, consider $dif(u) = \exp(-\sigma u^2)$; $\sigma > 0$.

With noisy image $g(x, y)$ as initial data, and homogeneous Neumann boundary conditions, march forward with

$$\begin{cases} w_t = \nabla \cdot \{dif(|\nabla w|)\nabla w\}, \\ w(x, y, 0) = g(x, y), \end{cases} \quad (2)$$

Results **visually similar** to TV denoising.

Image L^1 Lipschitz exponents α .

Measures **fine structure** in noise free image.

$g(x, y)$ has L^1 Lipschitz exponent α iff

$$** \int_{\mathbf{R}^2} |g(x+h_1, y+h_2) - g(x, y)| dx dy = O(|h|^\alpha), **$$

as $|h| \downarrow 0$, where $|h| = (h_1^2 + h_2^2)^{1/2}$, and α is fixed with $0 < \alpha \leq 1$.

$$g(x, y) \in BV(\mathbf{R}^2) \Rightarrow \alpha = 1 \quad !!$$

Most natural images have $\alpha < 0.6$, $\notin BV(\mathbf{R}^2)$!!

Display localized non differentiable sharp features and texture, in addition to edges. More fine structure \Rightarrow **smaller** Lip α .

How to find Lipschitz α for $g(x, y)$?

For fixed $\tau > 0$, define **Gaussian blur** operator G^τ by means of Fourier series

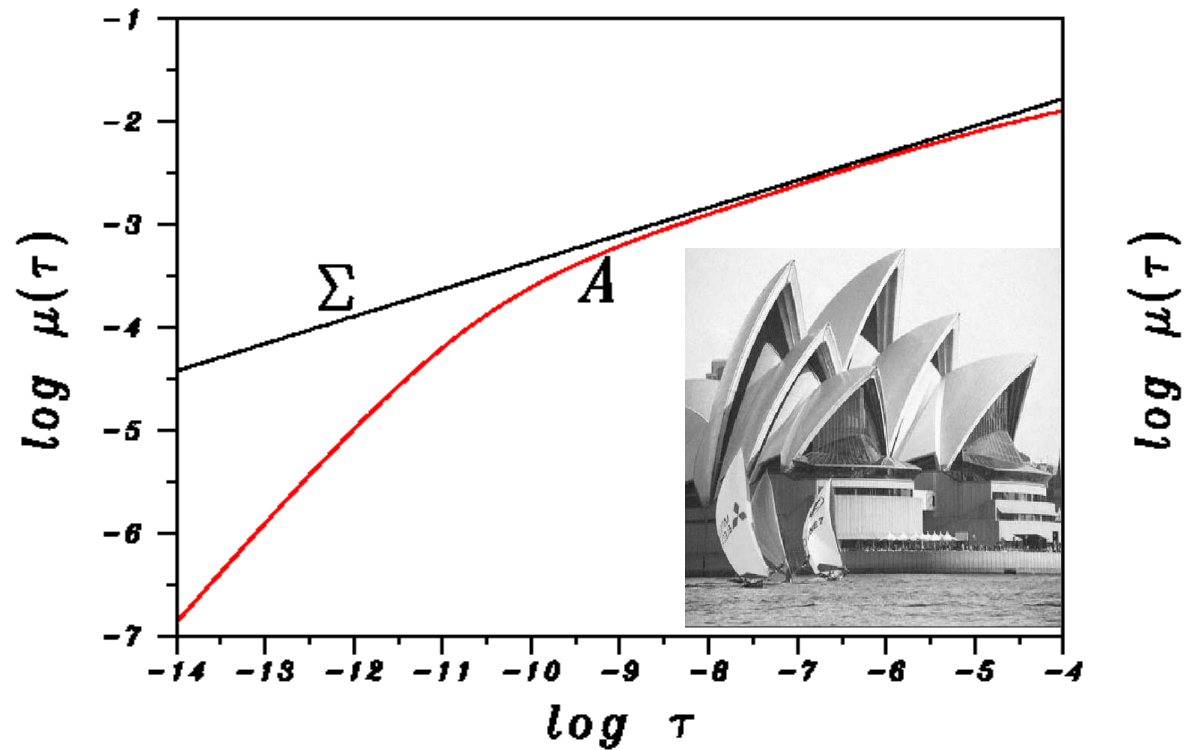
$$\{G^\tau g\}(x, y) = \sum_{-\infty}^{\infty} e^{-\tau(m^2+n^2)} \hat{g}_{mn} e^{2\pi i(xm+yn)}.$$

Let $\mu(\tau) = \|G^\tau g - g\|_1 / \|g\|_1$, $\tau > 0$.

Theorem (Taibleson, 1964). $g(x, y)$ has L^1 Lip α if and only if $\mu(\tau) = O(\tau^{\alpha/2})$ as $\tau \downarrow 0$.

Using FFT, compute $\mu(\tau_n)$ for sequence τ_n tending to zero, and plot $\mu(\tau_n)$ versus τ_n , on **log-log** scale. Locate positive constants C, α such that $\mu(\tau) \leq C \tau^{\alpha/2}$.

Estimating the Lipschitz exponent in Sydney image



Red curve is plot of $\mu(\tau)$ vs τ .

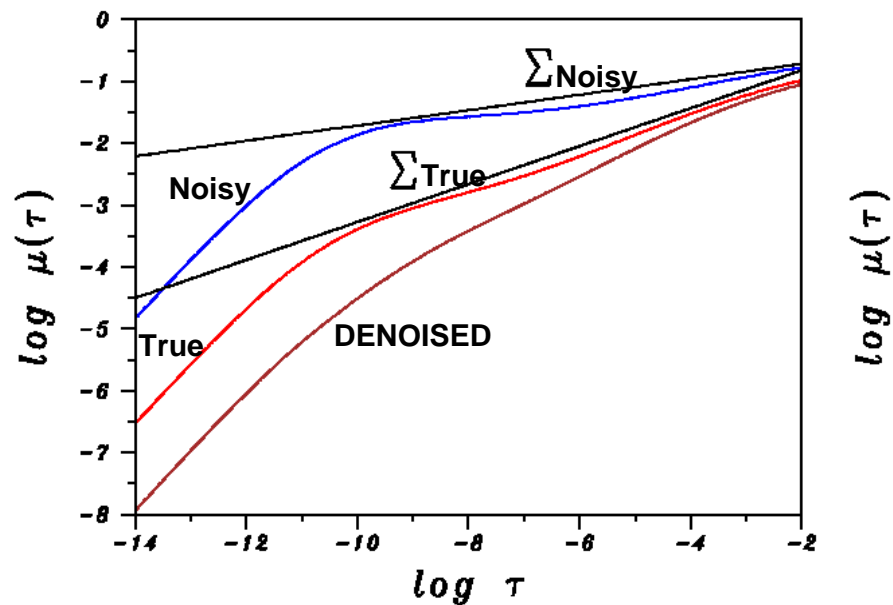
Lip $\alpha = 2 \times$ slope of majorizing Σ line.

Here, $\alpha = 0.530$

Adding noise **decreases** true image Lip α .
Some denoising methods eliminate texture,
and **increase** true image Lip α .



Lipschitz exponents after noising and denoising

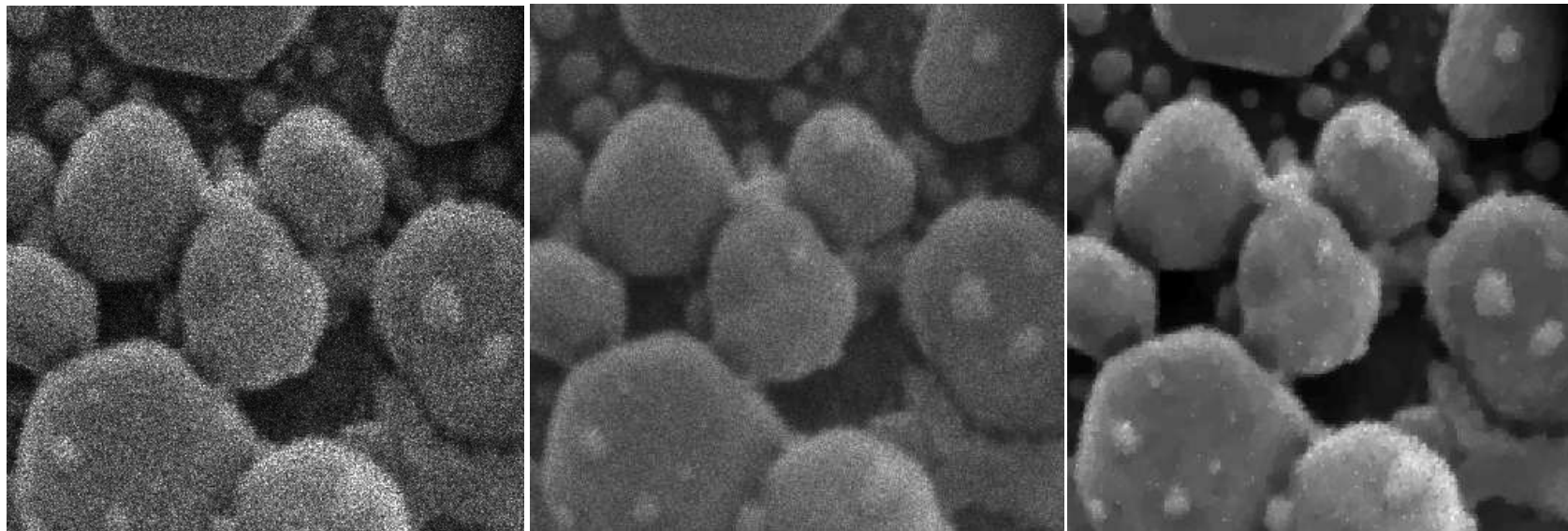


Fractional diffusion vs TV and Curvelet denoising

Noisy original detail

0.2 Fractional Diffusion

Split Bregman TV



<i>Image $f(x, y)$</i>	$\ f \ _1$	$\ \nabla f \ _1$	<i>Lip α</i>
Noisy original (300 nm)	74	47000	0.085
Frac diffusion ($\beta = 0.2, t^\dagger = 0.1$)	74	15000	0.211
Split Bregman TV ($\omega = 0.025$)	73	3500	0.697
Curvelet thresholding ($\sigma_n = 30$)	64	3000	0.704

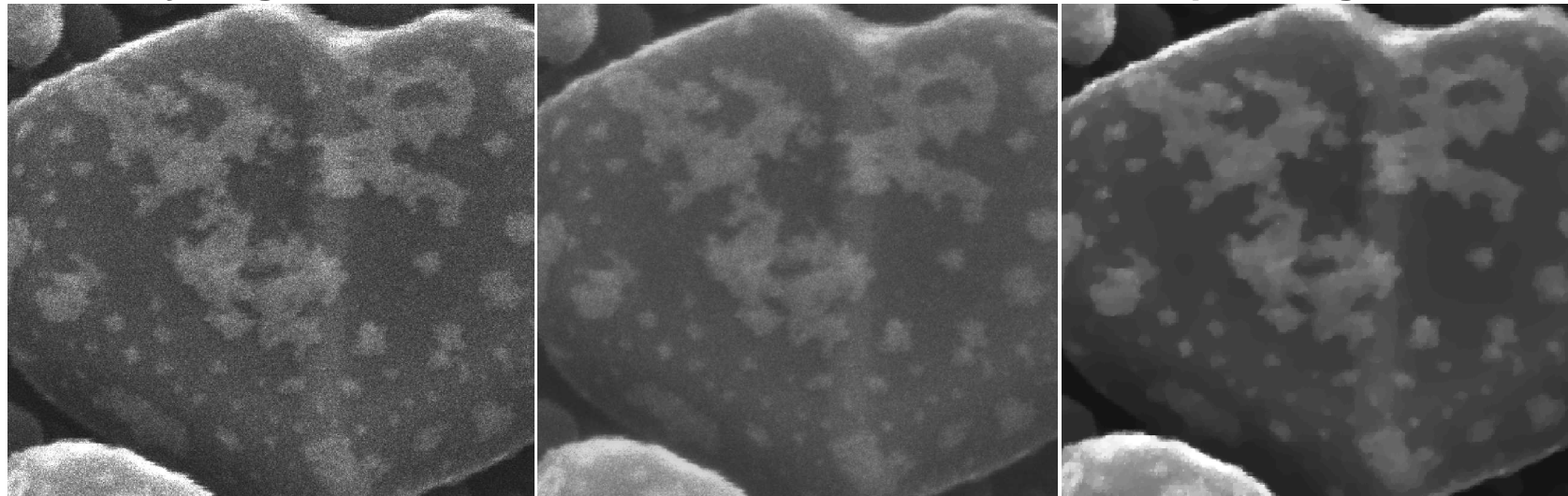
True surfaces may be fuzzy, like a **peach**, not smooth like an **apple**. Uncontrolled, **very severe** reductions in $\| \nabla g \|_1$ in TV and Curvelet images, versus **prescribed** reduction in $\| \nabla g \|_1$ in Fractional Diffusion image.

Fractional diffusion vs TV and Curvelet denoising

Noisy original detail

0.2 Fractional Diffusion

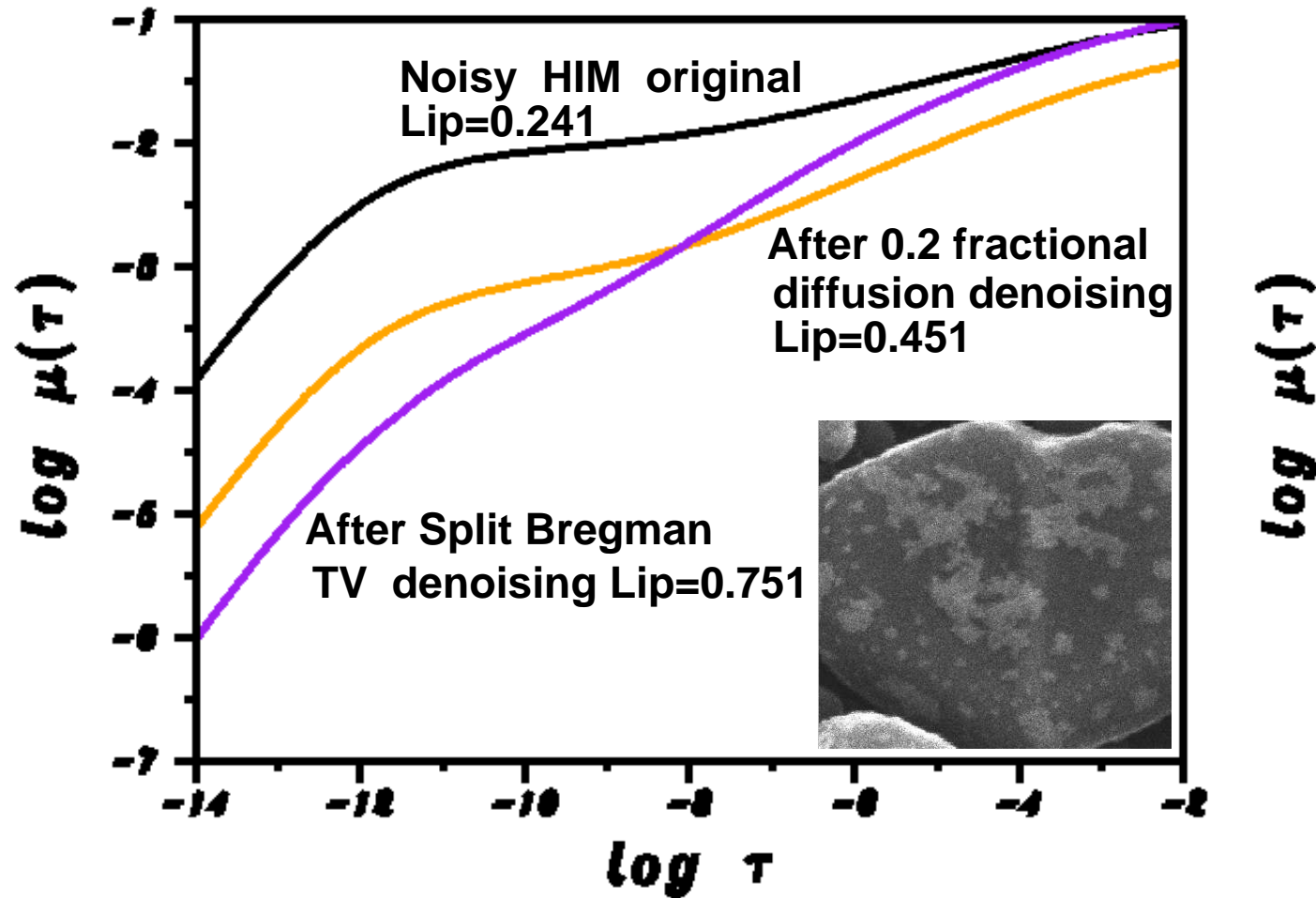
Split Bregman TV



<i>Image $f(x, y)$</i>	$\ f \ _1$	$\ \nabla f \ _1$	<i>Lip α</i>
Noisy original (600 nm)	88	25000	0.241
Frac diffusion ($\beta = 0.2, t^\dagger = 0.1$)	88	8500	0.451
Split Bregman TV ($\omega = 0.025$)	74	3400	0.751
Curvelet thresholding ($\sigma_n = 30$)	81	2700	0.810

Exit value of $\| \nabla g \|_1$ was **prescribed** in fractional diffusion, but not in TV or Curvelet denoising.

Behavior of Lipschitz exponents in HIM denoising



Study this HIM image with other evolution PDEs

What is special about fractional diffusion ?? Get same result with any PDE if prescribe exit $\| \nabla g \|_1$??

EQUIVALENT SMOOTHING EXPERIMENT

Compare short time smoothing using FIVE distinct parabolic evolution equations.

Prescribe identical exit value for $\| \nabla g \|_1$.

Perona-Malik; Marquina-Osher; Heat Equation; Fractional Diffusion $\beta = 0.2, \beta = 0.1$.

Study previous HIM image with exit $\| \nabla g \|_1 = 8500$.

Behavior of Lip α in denoised image ???

FRACTIONAL DIFFUSION IS SPECIAL !!!
Study equivalent smoothing with 5 PDEs

Exit Lipschitz exponent responds to fractional power of spatial operator in smoothing PDE !!

